Chemical Engineering Journal 428 (2022) 131013

Contents lists available at ScienceDirect

Chemical Engineering Journal

journal homepage: www.elsevier.com/locate/cej

Petrochemical condensate treatment by membrane aerated biofilm reactors: A pilot study

Irina Veleva [a,*], Wout Van Weert [a], Nicolaas Van Belzen [b], Emile Cornelissen [a,c,d], Arne Verliefde [a,d], Marjolein Vanoppen [a,d]

[a] PaInT, Particle and Interfacial Technology Group, Department of Green Chemistry and Technology, Faculty of Bioscience Engineering, Ghent University, Coupure Links 653, Ghent 9000, Belgium
[b] Dow Benelux BV, Herbert H. Dowweg 5, Hoek 4542 NM, Netherlands
[c] KWR Water Research Institute, Groningenhaven 7, Nieuwegein 3433 PE, Netherlands
[d] Centre for Advanced Process Technology for Urban Resource Recovery (CAPTURE), Belgium

ARTICLE INFO

Keywords:
MABR pilot in series
Real petrochemical condensate
Phenol
Organic acids
Process efficiency

ABSTRACT

An OxyMem membrane aerated biofilm reactor (MABR) pilot of two ~ 54 L reactors in series with a hydraulic retention time (HRT) of 10 h each was successfully applied for the treatment of real petrochemical condensate with a total organic carbon (TOC) concentration of ~ 100 mg/L. The main aim was to (i) evaluate the removal efficiency (RE) of main petrochemical pollutants and (ii) to examine the operational performance of the two on-site pilot-scale MABR units. The start-up/inoculation of the reactors in batch mode, followed by continuous pilot operation on synthetic feed, and the transition from synthetic to an actual petrochemical feed were covered. At stable operational conditions on the actual feed, the pilot in series achieved an overall RE for TOC, biological oxygen demand (BOD_5), organic acids, phenol, and ammonia of 80–85%, ~95%, >98%, ~98%, and 70–90%. The system in series demonstrated high resilience to process fluctuations, high treatment efficiency of the complex feed, and the ability to develop a diverse biofilm. In terms of oxygen transfer rate (OTR), oxygen transfer efficiency (OTE), and specific aeration efficiency (SAE) values of > 1.5 g/m^2/day, > 21%, and > 6.5 kg O_2/kWh were achieved. Such values outcompete the aeration efficiency (AE) of conventional activated sludge (CAS) processes and demonstrate the potential of MABRs to achieve higher OTE. Based on the collected data, the MABR concept in series can be considered highly effective for treatment of petrochemical streams.

1. Introduction

Petrochemical activities may lead to the formation of hazardous by-products such as oils, benzene toluene ethylbenzene and xylene (BTEX), phenols, and organic acids, which can end up in water sources. Being volatile, they can cause breathing problems and accumulate in the body as they are hardly biodegradable, leading to severe health consequences e.g., cancer [1,2]. The toxic effect of BTEX, phenol, and its derivatives is recognized worldwide and therefore petrochemical industries treat their wastewaters before safe discharge [2,3,4].

The biological degradation of such toxic pollutants to less harmful compounds in wastewater treatment plants (WWTPs) is normally sufficient and environmentally friendly [2,3,5,6]. Typically, CAS systems are aerated through air bubbling diffusors, which help with bulk mixing, but are energy intensive with low OTE (4–30%, standard conditions [7]). Such inefficiency requires excessive aeration, which can lead to stripping of volatile organic compounds (VOCs) [7,8,9,10,11,12].

Abbreviations: AOBs, Ammonia oxidizing bacteria; BOD_5, Biological oxygen demand after 5 days (mg/L); BTEX, Benzene, toluene, ethylbenzene, xylene (mg/L); C, Carbon; CAS, Conventional activated sludge process; COD, Chemical oxygen demand (mg/L); CSTR, Continuous stirred tank reactor; DO, Dissolved oxygen (mg/L); F/M, Food to microorganism ratio (kg BOD_5/kg MLSS/day); HMI, Human machine interface; HRT, Hydraulic retention time (h); HS GC–MS, Headspace gas chromatography - mass spectrometry; IC, Ion chromatography; LLD, Lower limit of detection (mg/L); MABR, Membrane aerated biofilm reactor; MLSS, Mixed liquid suspended solids (mg/L); M_{oxygen}, Molecular weight of oxygen (32 g/mol); N, Nitrogen; NDIR, Non-dispersive-infra-red; NOBs, Nitrite oxidizing bacteria; OAP, O-aminophenol (mg/L); P, Phosphorus; PDMS, Polydimethylsiloxane; PFR, Plug flow reactor; SF, Synthetic feed; SND, Simultaneous nitrification denitrification; TC, Total carbon (mg/L); TIC, Total inorganic carbon (mg/L); TN, Total nitrogen (mg/L); TOC, Total organic carbon (mg/L); VFA, Volatile fatty acids (mg/L); VOCs, Volatile organic carbons (mg/L); W, Week; WWTP, Wastewater treatment plant.

* Corresponding author.
E-mail address: Irina.Veleva@UGent.be (I. Veleva).

https://doi.org/10.1016/j.cej.2021.131013
Received 8 April 2021; Received in revised form 9 June 2021; Accepted 22 June 2021
Available online 8 July 2021

Nomenclature

Parameters used in the equations

$X(O_2)$	Fraction of oxygen in air of 0.21 (-)
115 200	Conversion factor from mol O_2/J to kg O_2/kWh
AE	Aeration efficiency (kg O_2/kWh)
A_m	Membrane area (m^2)
C_{in}	Influent concentration of the component of interest (mg/L; g/day)
COD_{feed}	The chemical oxygen demand load in the feed to R-1 (g COD_{feed}/m^2/day)
$COD_{removed,\ R\text{-}1}$	The chemical oxygen demand removed in R-1 (g $COD_{removed,\ R\text{-}1}/m^2$/day)
f	Fraction of transferred oxygen (-)
g TN_{feed}	The total nitrogen load in the feed to R-1 (g TN_{feed}/m^2/day)
g $TN_{removed,\ R\text{-}1}$	The total nitrogen removed in R-1 (g $TN_{removed,\ R\text{-}1}/m^2$/day)
J_{oxygen}	Oxygen flux (g/m^2/day)
$NH_3\text{-}N_{feed}$	The ammonia nitrogen load in the feed to R-1 (g $NH_3\text{-}N_{feed}/m^2$/day)
$NH_3\text{-}N_{removed,\ R\text{-}1}$	The ammonia nitrogen removed in R-1 (g $NH_3\text{-}N_{removed,\ R\text{-}1}/m^2$/day)
OTE	Oxygen transfer efficiency (%)
OTR	Oxygen transfer rate (g/m^2/day) – formulation used in the current study
Overall/total RE	Removal efficiency achieved by the pilot in series, R-1 + R-2
Q	Flow rate (L/h, L/day)
Q_{PF}	Process gas feed flow rate (m^3/h/m^2)
RE	Removal efficiency (%)
SAE	Specific, at process conditions, aeration efficiency (kg O_2/kWh)
v_m	Standard gas volume at standard temperature and pressure (0.0224 m^3/mol)
W*	Adiabatic compression energy (J/mol_{air})
X_F	Molar fraction of oxygen in the feed (-)

Other process limitations of the CAS system are the need for separate process steps for nitrification (aerobic) and denitrification (anaerobic) [8,10] and sufficient upstream buffering to prevent from shock loads of toxic compounds (e.g., phenol, methyl tertiary butyl ether) [8,13].

Compared to the CAS process, the MABR concept has shown potential for a more efficient oxygen supply [9,14,15]. An MABR uses hollow fiber membranes as (i) aerators, which are pressurized with the gas of interest, and (ii) as a support for biofilm attachment. Biomass formation on the surface of MABR membranes is a requirement for removal of chemical oxygen demand (COD) and N and for a desired and controllable microbial biofilm growth [16]. The flux of the supplied gas (e.g., O_2) across the membrane (i.e., OTR) is dictated by the biological demand - the higher the demand, the greater the driving force [5,10,14,17]. Thus, an MABR allows control over the air flowrate inside the membranes to achieve the highest OTE and AE and still reach the biological oxygen demand [14,18]. Depending on the process specifics, MABRs can reach OTE in the range of 20–100% [14,16,17,18,19,20].

In addition, unlike bubble-based aeration, MABR promotes a unique counter-current transport of electron donor and acceptor. This promotes the stratification of the biofilm, consisting of both aerobic autotrophs (e.g., ammonia oxidizing bacteria (AOBs) and nitrite oxidizing bacteria (NOBs)), aerobic heterotrophs and anaerobic heterotrophs (denitrifiers), thus allowing simultaneous nitrification and denitrification (SND, Fig. 1). Therefore, total nitrogen (TN) and COD can be removed in the same basin [10,14,16,21,22].

Under optimal conditions, the bubbleless aeration in MABRs can prevent the stripping of volatiles in petrochemical wastewaters [10,16,23,24]. The stratified biofilm also supports diverse communities with a higher tolerance to toxic shocks and inhibitory substances [22,25,26,27].This makes MABRs suitable for the treatment of high strength industrial streams and recalcitrant compounds [5,6,10,16,21]. For a background on bacterial biofilm analysis, the reader is referred to Klindworth et al. (2013) [28], Schloss et al., 2011 [29], Kozich et al., 2013 [30], and Cao et al. (2020) [31]. However, this is beyond the scope of the current work.

Li et al. (2015) [5] used a small-scale MABR to treat oil-field wastewater with COD, oil, NH_4^+-N, and TN concentration of 480 mg/L, 22.4 mg/L, 5.3 mg/L, and 31 mg/L and obtained RE of 82.3%, 85.7%, 32.1%, and 71.9%, respectively. In a study by Tian et al. (2019) [6], o-aminophenol (OAP, C_{feed} of 1179 mg/L) was removed via a lab-scale

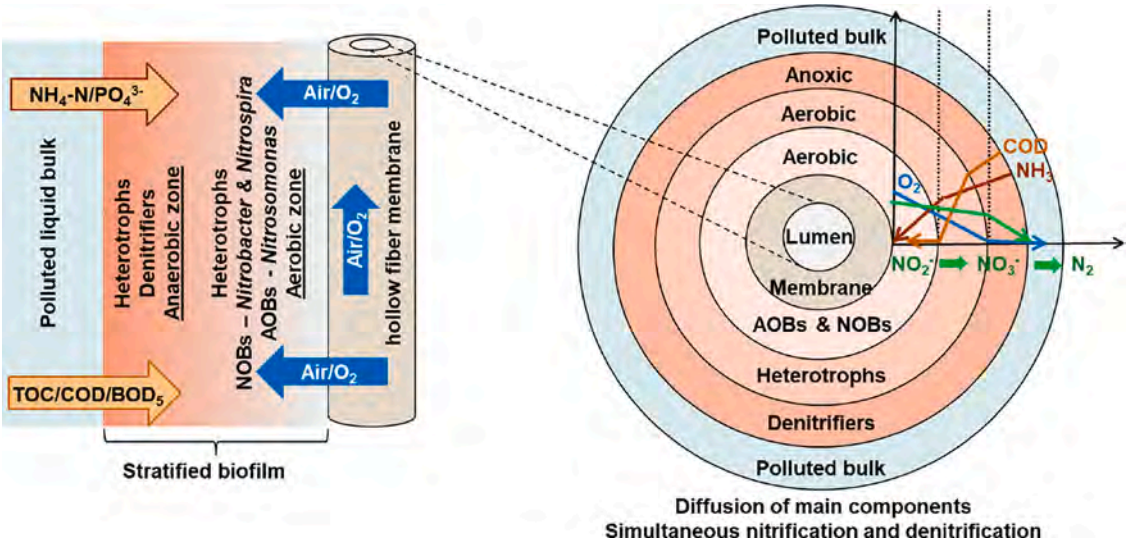

Fig. 1. Schematic representation of an MABR stratified biofilm (left side) and zoomed in diffusion profile of main components, biological activities, and simultaneous nitrification and denitrification (right side). Own figure.

MABR with an efficiency of > 99%. The same treatment approach was also applied for the removal of acetonitrile (load of 10.5 g/m^2/day) with RE ~ 97% and undetectable acetic acid in the effluent [24].

However, the majority of the reported research on MABRs is limited to lab-scale and a few pilot-scale cases. This highlights the need for extended pilot and full-scale research on MABR treatment of real (high strength) industrial streams with recalcitrant pollutants [16]. The advantage of a pilot-scale set-up lies in the improved comparability of the applied conditions to full-scale expectations, a more representative response to feed fluctuations and more reliable results for a long-term run. Furthermore, the evaluation of the energy demand is more realistic, and the synergy between parameters can be observed.

Therefore, the present research studies a pilot of two identical OxyMem MABRs in series. The pilot was started-up/inoculated in batch mode, then continuously operated on synthetic feed, and afterwards continuously operated on a real petrochemical condensate. The aim of this research was to (i) evaluate the removal efficiency of main petrochemical pollutants and (ii) to examine the operational performance of the two pilot-scale reactors. This study also aims to respond to the lack of sufficient long-term pilot MABR trials. To the best of our knowledge, the present study is the first to cover the treatment of a real petrochemical condensate through an MABR configuration at pilot-scale level.

2. Materials and methods

2.1. Composition of the real condensate stream

The condensate originated from the naphtha cracking process at a petrochemical site. The stream is polluted with phenol, organic acids, pyrolysis gasoline (aromatics, BTEX - Table A.1, Appendix A), added emulsion breakers, and C_9-C_{10} fractions. The stream is currently treated at the WWTP of the company.

Around 10 m^3 of the condensate from the production site was delivered to the MABR pilot. Due to logistic limitations and the elaborate sampling procedure in an explosion-sensitive area, the stream was periodically collected and stored in plastic vessels for a maximum of 8 – 10 weeks. Because of the prolonged storage, a slight variation in the initial composition (TOC, main pollutants, pH) of the condensate was detected. This could be related to an ongoing biological degradation in the storage tanks and was continuously monitored.

2.2. MABR pilot

2.2.1. Reactor and membrane characteristics

The condensate was treated in a pilot with two identical MABRs, later referred to as R-1 and R-2 (Fig. 2) and each was assumed to be a completely stirred tank reactor (CSTR). The pilot and the membranes were supplied by OxyMem DuPont (Athlon, Ireland). The two reactors were operated in series due to the projected higher performance and tolerance to shock loads. In such configuration, removal of multiple/competing contaminants (e.g., acetic acid and phenol [13]) in stages is expected as well [10,17].

In general, at an increasing number of CSTR's in series, it is expected that the configuration progressively resembles the performance of a plug flow reactor (PFR). Overall, the conversion rate in a PFR is projected to be higher than in a single CSTR, because of the higher average concentration or "no-back mixing" versus the complete mixing in a CSTR. This would lead also to an improved average reaction rate and higher effluent quality from a PFR [32].

Each reactor had an effective volume of ~ 54 L and a see-through polycarbonate structure for better visibility. The OxyMem membranes were made from polydimethylsiloxane (PDMS)/silicone material and were designed in a flow-through/open-end mode with a total surface area of 20 m^2/reactor. The specifics of the membranes are gathered in Table A.2, Appendix A.

2.2.1.1. Equipment and pilot specifications. The system had one main, Watson Marlow-Jason 30 universal, feeding pump, which introduced the influent condensate. The pilot was operated in series and the overflow of R-2 was considered to be the polished stream. Each MABR received pressurized air from a MEDO piston LA28b pump (Nitto Kohki Europe GMBH, Steinenbronn, Germany) and was continuously stirred via a LOWARA TLCN 25–2.5 (Dordrecht, The Netherlands) circulation pump.

To maintain optimal biofilm thickness, a scouring air blower (MEDO LA-60B, Nitto Kohki, Europe GMBH, Steinenbronn, Germany) was installed at the bottom of each MABR. In addition, an inlet/outlet gas flow and pressure meters, a reactor volume indicator, and an off-gas analyzer (O_2/CO_2) for the active reactor were placed. The temperature of the pilot was not regulated and thus corresponded to the ambient environment (15–22 °C). In the pilot, a human machine interface (HMI)

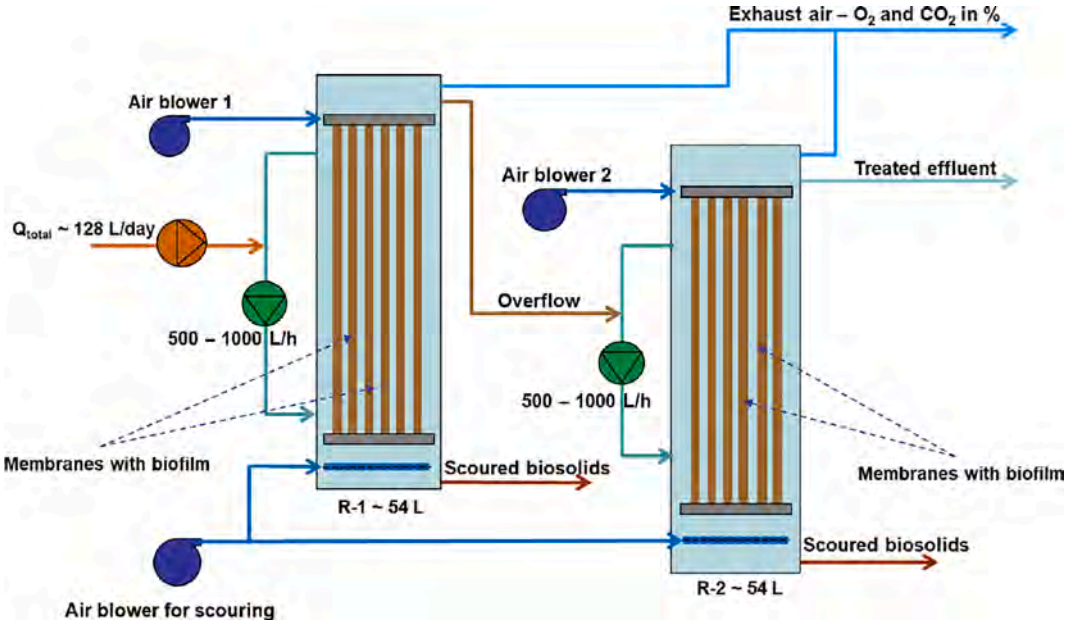

Fig. 2. Simplified scheme of the OxyMem MABR twin pilot in series. Own figure.

to monitor and log the main operational parameters was installed.

2.3. Start-up in batch mode and continuous operation on synthetic feed water with active R-1 and R-2 - period I

2.3.1. Start-up - inoculation in batch mode

Both MABRs were inoculated with ~ 53 L sludge from the WWTP on site, similar to previous MABR studies by Syron et al. (2015) [14] and Hanay et al. (2013) [27]. A food/microorganism (F/M) ratio of 0.1 kg BOD_5 per day/kg mixed liquid suspended solids (MLSS) was achieved, which resembled the measured F/M ratio at the full-scale CAS WWTP. To achieve an effective biofilm formation, the system was operated in batch mode in the first 4–5 days with a well-mixed bulk for sufficient contact between the biomass and the membranes.

2.3.1.1. Continuous operation. After these first few days, the system was switched to continuous operation. An HRT of 10 h per reactor was set, which is comparable to values reported in the literature [21,27]. To promote biomass acclimatization and the development of (amongst others) phenol consuming microorganism, the initial synthetic feed (SF) consisted of tap water, 25% of the average acetate, and 1 – 5% of the average phenol concentration in the real condensate (Table A.1, Appendix A). Next, the acetate concentration was gradually increased in 25% increments and in week 4, approximately 5% of the average propionate concentration in the real condensate was also introduced. From that point on, the added amount of phenol and propionate in the feed were also increased in 25% increments. After each increase, the concentrations were maintained for one week. For sufficient contact between the supplied constituents/bulk liquid and the biofilm, a mixing flow rate of ~ 1000 L/h or 10% of the process HRT was implemented. At this setting, a complete turnover of each reactor was achieved every 6^{th} minute.

This feeding mode was maintained until the three main carbon constituents (acetate, propionate, and phenol (Table 1)) gradually reached their full condensate concentrations (Table A.1, Appendix A). The average composition of the feed during period I is shown in Table A.7, Appendix A. This approach was applied during the first eleven weeks to minimize the shock on the biomass and to secure the biofilm formation. During the development of the biofilm, scouring of the membranes was avoided for an optimal growth and stratification. After the first four weeks, the biofilm was scoured once per week for 1-minute to control its thickness.

Due to the limited amount of macro and micronutrients in the real condensate, these were added throughout the whole trial to promote the growth of a functional biofilm. Based on the optimal ratio for carbon (BOD_5/C): nitrogen (N): phosphorus (P) of 100:5:1 reported in literature [33,34,35] and given the expected load of 12.80 g BOD_5/day (Table A.1, Appendix A), a daily dosage of N and P of 0.64 g/day and 0.13 g/day was calculated. For a better response of the system to unexpected peak loads, a safety factor of three was used.

Based on these calculated values, a synthetic mixture with NH_4Cl of 7.4 g/L, KH_2PO_4 of 1.7 g/L and 1.25 μL/L of the micronutrients (Ni, Zn, Cu, etc.) Stabilox mixture GC M220 (AVECOM NV, Industrieweg 122P, B-9032 Wondelgem, Belgium) was made. The nutrient solution was continuously dosed into the feed line with a $Q_{nutrients}$ of ~ 1 L/day, which together with the synthetic carbon mixture (Q_{feed} of ~ 127 L/day) resulted into a Q_{total} of ~ 128 L/day (Table A.2, Appendix A).

2.4. Transition from continuous synthetic feed to only real petrochemical condensate, mainly R-1 active - period II

After 3 weeks of operation at 100% dosing of all constituents (Table 1), the SF was gradually replaced by the real condensate from the crackers. The following transition was chosen per week (W): W12 (75%, SF + 25%, condensate); W13 (50%, SF + 50%, condensate); W14 (25%, SF + 75%, condensate) and W15 (0%, SF + 100%, condensate). From this point onwards, the system was continuously supplied only with real petrochemical condensate (from now on referred to as period II). Because of insufficient easily biodegradable carbon in the condensate, the biofilm in R-2 died and this unit was biologically unactive for the majority of this period. The average composition of the feed during period II was summarized in Table A.7, Appendix A.

2.5. Continuous operation only on real petrochemical condensate, R-1 and R-2 active – Period III

During period III, the system was fed only with real condensate and R-2 was re-started by refilling 50% of it with tap water and 50% with overflow from R-1 after scouring. In this stage, both reactors were active and functional. The average feed composition to the pilot during period III was tabulated in Table A.7, Appendix A.

2.6. Sampling

Samples for analyses were taken from the feed mixtures and the reactors. Both MABRs were considered completely mixed and grab samples from the bulk were taken. Once the organic acids and phenol were removed to effluent levels close to their corresponding lower limit of detection (LLD), the sampling frequency was increased to once or twice per week.

2.7. Analytical methodology

To protect the analytical equipment, the collected samples were filtered using a 0.45 μm (SPARTAN™, Whatman™, United Kingdom) filter before analysis for TOC, organic acids, phenol, ammonia, and phosphate.

2.7.1. TOC

To determine the TOC content of the samples, the total inorganic carbon (TIC) was subtracted from the total carbon (TC, organic and inorganic) content. TC and TIC were quantified in a non-dispersive-infra-red (NDIR) gas analyzer (Shimadzu, TOC-L CPH/CPN, Kyoto, Japan). The LLD of the equipment was 1 mg/L. Reference method NEN-EN 1484 [36]. For more details see section B.1, Appendix B.

2.7.2. TN, NH_3, NO_2^- NO_3^-, and PO_4^{3-}

TN was determined by the TNM-L total nitrogen unit which is an additional chemiluminescence based detector on the Shimadzu TOC-L instrument. Reference method: NEN-EN 12260:2003 [37]. For more details see section B.2, Appendix B.

The ammonia/ammonium (LCK-304, 0.015–2.0 mg/L NH_4^+-N or

Table 1
Composition of the synthetic feed – gradual increase in carbon dosage.

Compounds	Weeks from the start-up										
	W1	W2	W3	W4	W5	W6	W7	W8	W9	W10	W11
Acetate (%)	25	50	75	100							
Phenol (%)	1	1	1	5	25	25	50	75	100		
Propionate (%)	0	0	0	5	25	25	100				

W - stands for week.

0.02–2.50 mg/L NH_4^+, HACH Lange GMBH, Germany) and orthophosphate (LCK-349, 0.05–1.50 mg/L PO_4-P, 0.15–4.50 mg/L PO_4^{3-} or 0.15–3.50 mg/L P_2O_5, HACH Lange GMBH, Germany) in the samples were analyzed with a HACH DR3900 VIS (Tiel, The Netherlands) spectrophotometer. The detection methods for these components were validated within the company for streams with a complex petrochemical matrix. Due to that, the LLD for both compounds differed from the HACH specifications and were defined as 0.3 mg/L. In the present study, the collected results (sum of NH_4^+ and dissolved NH_3) were reported as NH_3 in mg/L.

The amount of NO_2^- and NO_3^- was determined through ion chromatography (IC) using a Thermo ICS-2100 system with LLD of 0.2 mg/L.

2.7.3. Organic acids, phenol, BOD_5, BTEX, and COD

The concentration of organic acids was determined using a Dionex ICS-5000 (Sunnyvale, USA) IC with an Ion Pac AS15 column. The LLD of the equipment was 1 mg/L.

The amount of phenol in the samples was determined spectrophotometrically with an LCK-345 kit (0.05–5 mg/L, HACH, Lange GMBH, Germany) with a LLD of 0.2 mg/L. For more concentrated samples, an LCK-346 (HACH, Lange GMBH, Germany) with a higher measuring range (5–50 mg/L and 20–150 mg/L) was used.

The COD in the condensate was measured spectrophotometrically using a cuvette-based test LCK-314 (15–150 mg/L, HACH, Lange GMBH, Germany) and a DR3900 spectrophotometer (HACH, Germany). The BOD after 5 days was defined based on the NEN-EN-1899–1 method [38]. The fractions of BTEX measured in the real condensate were detected via headspace gas chromatography - mass spectrometry analysis (HS GC–MS).

2.7.4. Dissolved oxygen (DO), pH, and conductivity

The DO in the system was detected through a HACH, HQ30D Portable Dissolved Oxygen Meter, Laboratory Kit for Water. The pH and the conductivity of the samples were measured via a multimeter METTLER TOLEDO, Seven Excellence™.

$$Removal\ efficiency = \left(\frac{C_{in} - C_{out}}{C_{in}}\right)100 \quad (1)$$

The OTR (g O_2/day) dictated by the biofilm of the pilot was calculated using eq. (2) – adapted from Côté et. al. (2015) [18].

$$Oxygen\ transfer\ rate = J_{oxygen}.A_m \quad (2)$$

Where J_{oxygen} is the oxygen flux (g O_2/m^2/day); A_m is the membrane area (m^2). The oxygen flux (J_{oxygen}) in the system was calculated based on the equation described in Côté et al. (2015) [18].

The OTE (%) of the MABR pilot was calculated as follows [18].

$$Oxygen\ transfer\ efficiency = \frac{J_{oxygen}}{24}\frac{V_m}{Q_{PF}.M_{oxygen}.X_F} \quad (3)$$

Where J_{oxygen} (g/m^2/day) is the oxygen flux; Q_{PF} is the process gas feed flow rate in $m^3/h/m^2$; V_m is the standard gas volume at standard temperature and pressure (0.0224 m^3/mol); M_{oxygen} is the oxygen molecular weight (32 g/mol); X_F is the molar fraction of oxygen in the feed (-).

The SAE (kg O_2/kWh) was calculated based on eq. (4) [39].

$$Specific\ aeration\ efficiency = 115\ 200.\frac{X(O_2)f}{W^*} \quad (4)$$

In eq. (4), W^* is the adiabatic compression energy (J/mol_{air}). In order to correlate it to the amount of O_2, the fraction of oxygen in air $X(O_2)$of 0.21 (-) and f, the fraction of transferred oxygen (-), were considered. To convert the obtained mol O_2/J to kg O_2/kWh a conversion factor of 115 200 was used.

To calculate the theoretical oxygen demand in R-1 (g O_2/m^2/day), eq. (5) was applied. The COD (g COD_{feed}/m^2/day) and ammonia nitrogen (g NH_3-N_{feed}/m^2/day) load to R-1 were considered. To define the theoretically needed oxygen, oxidation ratios of 1 (k)gO_2/ 1 (k)g COD [40], 5 g COD/g $N_{removed,\ denitrification}$ [18], and 4.57 g O_2/ $N_{removed,\ nitrification}$ [14,18,19,41] were implemented. More detailed data is gathered in Table A.6, Appendix A.

$$Theoretical\ oxygen\ demand,\ R-1 = \left(\frac{gCOD_{feed}}{m^2.day} - \frac{5gCOD}{gN_{removed,denitrification}}.\frac{gTN_{feed}}{m^2.day}.RE_{TN,R-1}\right)\frac{1gO_2}{1gCOD} + \frac{gNH_3 - N_{feed}}{m^2.day}.\frac{4.57gO_2}{gNH_3 - N} \quad (5)$$

2.8. Calculations

The RE (%) achieved by the MABR installation was calculated using equation (1). The RE achieved by the system in series (R-1 + R-2) is defined and later on referred to as the overall/total RE. The load of each component to the pilot was calculated based on the membrane area of R-1 only (20 m^2 - Table A.2, Appendix A). Depending on the feed composition and the performance of R-1 or the pilot in series (R-1 + R-2), the main pollutants were often removed to below the LLD. In these cases, the RE was calculated by accepting the LLD as the value achieved by the system.

To define the N removed in the process through denitrification, a TN balance was made, accounting for the amount of TN in the feed to R-1 (g TN_{feed}/m^2/day), including the externally added NH_3-N, and the measured values in R-1 (Table A.6, Appendix A). Since TN consist of all N fractions (organic, inorganic, NO_x) present in the stream, it is expected that a decrease in this parameter after denitrification refers to N_2 losses to the atmosphere [7].

To calculate the theoretical oxygen demand of R-2, eq. (6) was applied. In this equation, the same terms as the ones described in eq. (5) were implemented and the performance of R-1 (RE_{COD}, $RE_{NH3\text{-}N}$, and RE_{TN}) and R-2 (RE_{TN}) was incorporated. The obtained data was tabulated in Table A.6, Appendix A.

$$Theoretical\ oxygen\ demand, R-2 = \left(\frac{gCOD_{feed} - gCOD_{removed,R-1}}{m^2day} - \frac{5gCOD}{gN_{removed,denitrification}}.\frac{gTN_{feed} - gTN_{removed,R-1}}{m^2.day}.RE_{TN,R-2}\right)\frac{1gO_2}{1gCOD} + \frac{gNH_3 - N_{feed} - NH_3 - N_{removed,R-1}}{m^2day}.\frac{4.57gO_2}{gNH_3 - N} \quad (6)$$

2.9. Statistics

Values reported with standard deviation represent the mean of a certain parameter and its standard deviation calculated with the excel function STDEV.P.

3. Results and discussion

3.1. Performance of the MABR pilot during start-up in batch mode – period I

The first 4–5 days of batch mode indicated the initiation of biofilm development. Since the surface of the membranes was not completely covered, a high oxygen transfer to the bulk and lower resistance/high mixing flow rates were observed. This led to comparable ranges of the main process parameters for both reactors (Table 2), which could be directly linked to the simultaneous start-up of biological activity. This confirms findings of Côté et al. (2015) [18] and Kunetz et al. (2016) [41] where initial DO_{bulk} values near saturation, 8.5 mg/L [7,41] – 10 mg/L [41,42], were detected in an MABR.

3.2. Performance of the pilot on continuous feed: synthetic - period I, transition to petrochemical condensate – part of period II, and only petrochemical condensate feed - period II and III

3.2.1. TOC and BOD_5

While the system was continuously fed with SF (period I), the TOC load within this period was calculated, but not measured. During this period (Fig. 3) most of the TOC was removed primarily by R-1 with RE of 80–98%. This is in consistence with findings of Tian et al. (2019) [6] ($COD_{synthetic\ feed,\ OAP}$ of 367 mg/L, RE_{COD} of 97.1%) and Mei et al. (2019) [26] ($COD_{synthetic\ feed,\ p\text{-}nitrophenol}$ of 800 mg/L, RE_{COD} of 82%) obtained via a single MABR.

On the other hand, a decrease in the RE_{TOC} of R-1 to 30% and 60% was noted around days 15–35, and day 78 (period I, Fig. 3). In period I, also the BOD_5 feed content fluctuated largely (from 80 mg/L to 220 mg/L), resulting in large variations in the RE_{BOD5} (from 98% to a minimum of 25%, Fig. 4). This could be explained with an unexpected increase in the carbon content of the SF leading to a noticeable acute toxicity to the heterotrophs. Throughout these occasions, both reactors in series were still able to achieve an overall $RE_{TOC/BOD5}$ of 97–99%. This demonstrated the additional treatment capacity of the second reactor (see section 2.2.1).

Furthermore, the transition from the SF to the real condensate (days 80–98, Fig. 3, beginning of period II) did not cause any visible disruption in the behavior and RE of R-1. On the other hand, because of the feed biodegradation over time (see section 2.1) the TOC load gradually

Table 2
Main parameters detected during the first 4–5 days in batch mode.

Reactors	DO_{bulk} (mg/L)	pH	Conductivity (μS/cm)	Air flow (L/h)	Mixing (L/h)	Pressure (mbars)	O_2/CO_2 (%)
R-1	5.9	7.6	894	13.6	1173	157	19/0
R-2	6.8	7.9	862	13.6	1145	148	19/0

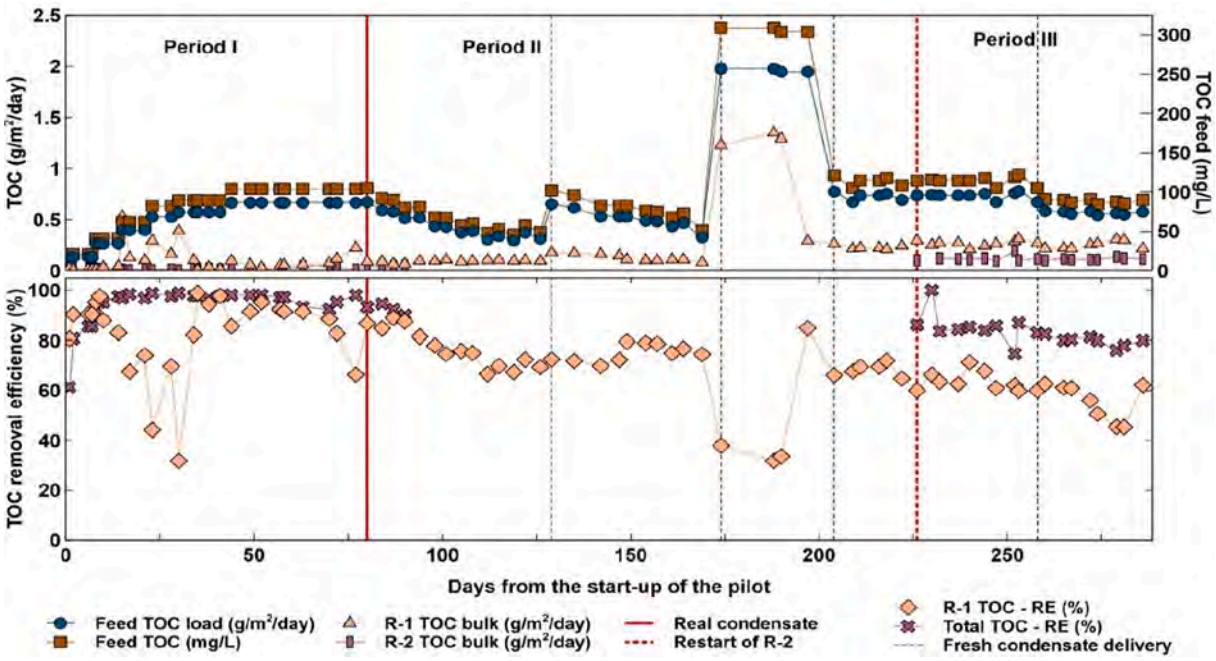

Fig. 3. Feed TOC concentration, TOC load to the MABR pilot in series, reactor's bulk values and TOC removal efficiency versus time from the start-up of the system.

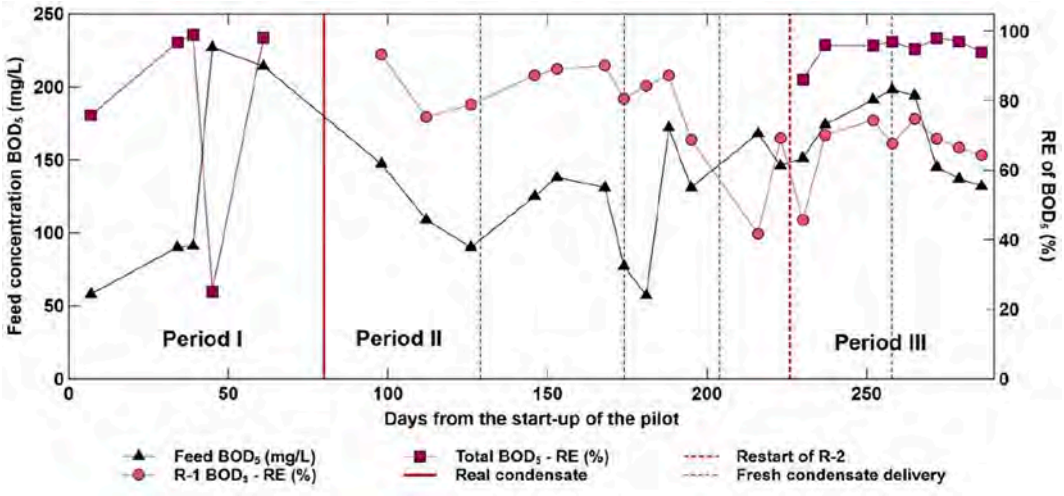

Fig. 4. BOD_5 concentration in the feed to the MABR pilot in series and removal efficiency over time from the start-up of the system.

decreased and ultimately caused biofilm loss in R-2 (period II, Fig. 3). Hence, at the applied feeding load and HRT (10 h) R-2 was defined as substrate limited with scarce biofilm although it can offer additional treatment at higher loadings. In general, to maintain the biofilm in R-2 a small fraction of the feed/easily biodegradable carbon could be directly fed into R-2. This feeding approach was not tested in the frame of the current study, but it was applied by Stricker et al. (2011) [17].

During the continuous operation only with real condensate (period – II) due to the biodegradation in the storage vessels each fresh delivery caused an occasional TOC spike. For instance, around day 129 (Fig. 3) a new condensate delivery led to an increase in the feed TOC from 49 mg/L (0.32 g TOC/m^2/day) to 102 mg/L (0.65 g TOC/m^2/day). This also doubled the amount of TOC in the effluent of R-1, from 15 mg/L to 28 mg/L. At both feed concentrations the RE of R-1 was ~ 70%.

With the next condensate delivery (day 174 - period II) a substantial peak in the feed TOC, ~300 mg/L (1.9 g/m^2/day), originating from unknown pollutants in the transportation vehicle was detected. R-1 was fed with this stream for 14 days and eventually achieved RE of TOC, organic acids, and phenol of ~ 85%, below the LLD, and equal to the LLD. On the other hand, the polluted feed had a substantially lower biodegradability and the feed BOD_5 dropped from ~ 121 ± 19 mg/L to 67 ± 10 mg/L. Nonetheless, the RE_{BOD5} in R-1 remained comparable at both BOD_5 concentrations, 86 ± 5% and 82 ± 2%, and to the RE_{TOC}. This could be due to the lack of acute inhibition of the contaminated condensate on the heterotrophs, which are known to be less sensitive e.g., than autotrophic nitrifiers [7]. Afterwards, a fresh condensate to replace the polluted feed was delivered.

The higher TOC in the fresh feed to R-1 and in its effluent (RE_{TOC} 40–70%) was linked to the presence of hardly or even non-biodegradable components for one reactor (period III, Fig. 3). This allowed the restart of R-2 and the achievement of a total RE_{TOC} of 80–85%, ~60% in R-1 and ~ 20% in R-2 (corroborated by Stricker at al. (2011) [17]). The overall/total RE_{TOC} (~80%) was presumably attributed to the removal of short chain organics, while the remaining were difficult to degrade (corroborated by P. Li et al (2015) [5]). Nonetheless, there must be enough easily biodegradable TOC to maintain the activity in both units.

During period III, an average feed BOD_5 of 165 ± 26 mg/L was detected with REs of 67 ± 9% achieved in R-1 and 95 ± 4% in total (R-1 + R-2). This evidently once again confirmed the advanced performance of the system in sequence. These findings are comparable to findings of Stricker at al. (2011) [17] obtained in a pilot of three sequenced MABRs ($C_{synthetic\ industrial\ feed,\ BOD5}$ ~ 2031 mg/L, RE_{BOD5} of ~ 99%).

3.2.2. Organic acids

The first four weeks of operation were dedicated to the development of the biofilm and analysis of the feed/removed acids were not performed. Afterwards, during period I (W5 to W11, Table 3) the MABRs in series removed the treated organic acids below the IC LLD of 1 mg/L. This corresponded to an overall RE of > 96%. Within the transition from synthetic feed to real condensate (W13 to W15, period II - Table 3) due to the lower feed TOC/inactive R-2 (see section 3.2.1) data for the removal of acids in R-2 was unavailable. On the other hand, R-1 was still able to remove the detected acids to below the IC LLD.

Table 3
Concentration of organic acids - continuous operation on synthetic feed (R-1 and R-2 active - period I) and transitional period from synthetic feed to real condensate (only R-1 active - period II).

Periods	Weeks from start-up	Concentration of acids (mg/L)								
		Acetate			Propionate			Formate		
		Feed	R-1	R-2	Feed	R-1	R-2	Feed	R-1	R-2
period I	5	x	x	x	x	x	x	x	x	x
	6	x	x	x	x	x	x	x	x	x
	7	x	x	x	x	x	x	x	x	x
	8	270	x	x	38	x	x	x	x	x
	9	201	<1	<1	25	<1	<1	x	x	x
	10	205	7	<1	37	<1	<1	x	x	x
	11	239	<1	<1	36	<1	<1	x	x	x
transition period II	13	102	~7	<1	23	<1	<1	9	<1	<1
	14	58	<1	*	13	<1	*	6.5	<1	*
	15	~45	<1	*	~5	x	*	~2	<1	*

x - data not available; * - R-2 loss of biofilm due to low feed TOC; data for W12 is not available.

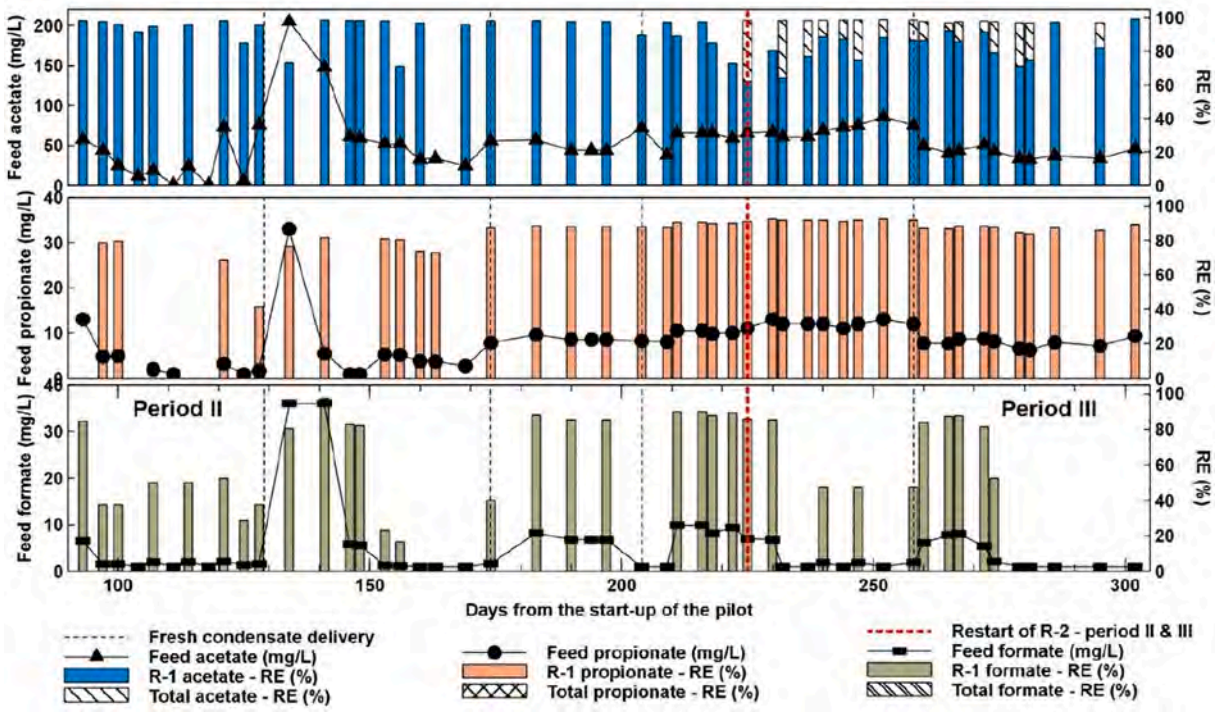

Fig. 5. Feed concentration of acetate, propionate, and formate and removal efficiency of the acids by the MABR pilot in series versus time after the transition from synthetic to real condensate only.

During period II (R-1 active) and III (R-1 and R-2 active) the system continuously treated only the real petrochemical condensate. In terms of acetic acid removal, until day 209 R-1 achieved an average RE of 94 ± 8% (period II, Fig. 5). Once the feed acetate rose from an average of ~ 40 mg/L to ~ 57 mg/L the efficiency of R-1 dropped to ~ 84 ± 10%. This, together with the increased feed TOC (from 74 mg/L to 105 mg/L, Fig. 3), allowed the restart of R-2. Thereafter, the system in series reached an average overall $RE_{acetate}$ of 98 ± 1% and demonstrated the advantage of the second reactor (period III, Fig. 5).

This corroborates findings of T. Li et al. (2008) [24] from a lab-scale MABR with $RE_{synthetic\ feed,\ acetonitrile}$ of 100% (~11.29 g/m^2/day) and no detectable acetic acid as byproduct. The current outcomes are also comparable with finding of P. Li et al. (2015) [5] from a single MABR with $RE_{volatile\ fatty\ acids\ (VFA)}$ ~ 80% ($C_{real\ oil\text{-}field\ wastewater,\ VFA}$ of 20 mg/L).

In all effluent samples for period II and III (Fig. 5) the measured values for propionate and formate were below the IC LLD. Occasionally, a low feed concentration of propionate and formate was detected, which led to low REs of > 42% and > 17%, but rather high actual performance of the pilot. Overall, R-1 was able to remove the propionate and formate below the IC LLD.

The only peak of the three acids in the feed was noted around day 134, period II. In this period, also an increase in the TOC load was observed (from 0.3 g TOC/m^2/day to 0.6 g TOC/m^2/day) associated with the delivery of a fresh condensate and variations in the petrochemical plant. In comparison with the previously detected feed values of acetate, propionate, and formate they were on average 4.4, 4.8, and 18-fold higher, respectively. Based on the collected data (Fig. 5), it can be concluded that even at such acute increase R-1 was able to achieve REs of 73%, 76%, and 80%, respectively. Once the feed composition normalized, R-1 achieved effluent values for the three acids below the IC LLD.

Such disturbances can be essential to define the maximum organic loading capacity of the system, its response to shock loads, and to mimic feed fluctuations often experienced at full-scale processes (corroborated by Stricker et al. (2011) [17]). The observed REs can be linked to the high diversity and subsequent resilience of the stratified biofilm to toxins and feed shocks, a main feature of the MABR concept [6,43].

3.2.3. Phenol

The first 4 weeks of the piloting were focused on the establishment of biofilm and the RE_{phenol} was not monitored. For the remainder of period I, the pilot achieved an overall RE_{phenol} of > 97% (Fig. 6). During period II, the removal of phenol was mainly conducted in R-1 because of insufficient easily biodegradable carbon to maintain R-2 (see section 3.2.1). Throughout this phase, R-1 achieved RE_{phenol} of 95 ± 7% ($C_{feed,\ phenol}$ of 24 ± 9 mg/L) which gradually dropped to 73 ± 15% when its feed concentration rose to 35 ± 8 mg/L. Similarly, Hanay et. al (2014) [27] reported that the increase of phenol, from 10 to 50 mg/L, in a synthetic feed to an MABR (HRT of 2.5 h) lowered the RE_{phenol} from ~ 100% to ~ 26–84%. The comparable response to higher feed phenol noted in the present study at much longer HRT (10 h/reactor) could be linked to the greater complexity of the real petrochemical condensate.

Besides that, during period II only one dip in the feed phenol was observed from 27 ± 1 mg/L to 3.5 mg/L, which unexpectedly also lowered the RE_{phenol} from 98 ± 1% to 79 ± 1% (Fig. 6). This fluctuation could not be explained based on the collected data and observations.

In the course of period III, a general decrease in the RE_{phenol} in R-1 was observed. This might be an indication for insufficient biomass or too thick biofilm, which hampers the diffusion or be a result of phenol toxicity due to its higher feed concentration. Together, both reactors achieved a total RE_{phenol} of 98 ± 2% (period III, Fig. 6) demonstrating the superior performance of the system in series. In contrast, Tian et. al (2019) [6] reported $RE_{synthetic\ feed,\ OAP}$ of > 99% exclusively via MABR-1 treating 203 mg/L (HRT of 14 h) and treating 1179 mg/L (HRT of 32 h). Similarly, Mei et al. (2019) [26] and Potvin et al. (2012) [44] described high $RE_{p\text{-}nitrophenol}$ (~80%, $C_{feed,\ p\text{-}nitrophenol}$ of 500 mg/L, HRT of 19 h) and significant $RE_{tetrabromobisphenol\ A}$ (~65%, C_{feed} of 125 ng/L, HRT of 2.4 h) from synthetic wastewater through a single MABR.

The difference between the achieved REs of highly toxic compounds in a single MABR compared with the obtained data in the current report can be traced to the contaminated stream. In all the above-mentioned

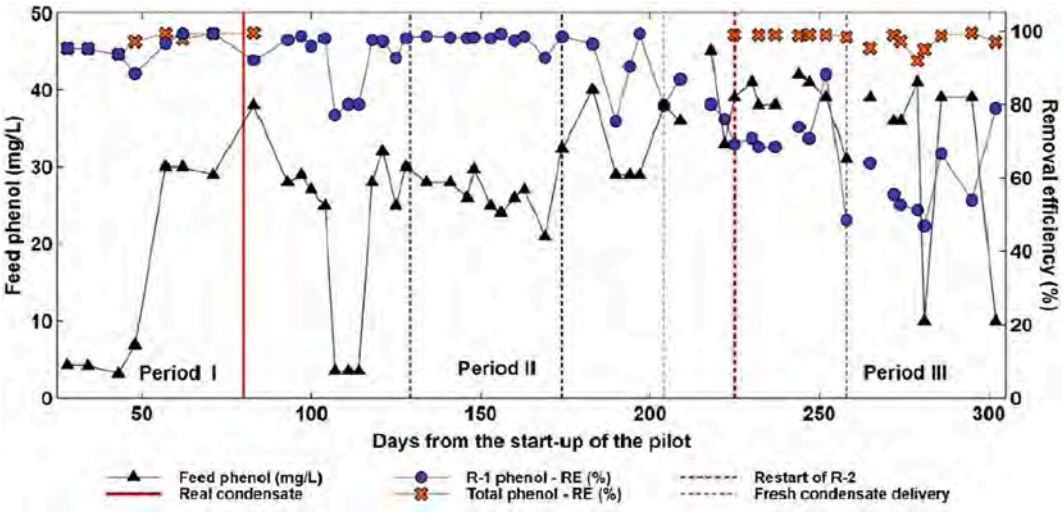

Fig. 6. Feed phenol concentration and removal efficiency of the MABR pilot in series versus time after the first four weeks from the start-up of the pilot.

studies [6,27,26,44], a synthetic feed was treated at either higher HRT or with less complex composition.

Generally, based on the outcomes from the present study, it can be concluded that the MABR is an efficient treatment approach for more resistant and inhibitory pollutants such as phenol.

3.3. Removal of nutrients

3.3.1. Ammonia removal, nitrification/denitrification, and DO profile

In general, even though the system experienced different operational fluctuations and shocks within period I, the pilot achieved a total $RE_{ammonia}$ of 90 ± 12% (Fig. 7).

During period I, the reduced RE of TOC (Fig. 3) and BOD_5 (Fig. 4) could be due to an inhibiting toxicity. This can also be the reason for the sharp deterioration in the $RE_{ammonia}$ in R-1, from ~ 100% to ~ 20%, observed in this period (Fig. 7). This corroborates findings by Navada et al. (2020) [45] where acute carbon toxicity to nitrification was detected. Tian et al. (2019) [6] and Barthe et al. (2015) [8] also reported the hindering effect of toxic/hardly biodegradable organics on denitrification and nitrification (phenol of 20–50 mg/L [8]), respectively.

Through period I, a buildup of NO_2^- and NO_3^- in R-1 and R-2 also occurred due to the suspected inhibition. The lower overall RE_{BOD5} (period I, Fig. 4) could also be related to a biomass decay and explain the high amount of free O_2/uncovered membranes in R-2 (Fig. 8).

In general, because denitrifiers are facultative aerobes (O_2 electron acceptor - highest energy quantity [7]), SND in one tank is possible but is defined as unpredictable [46]. Denitrifiers can also switch to anaerobic respiration in oxygen depleted environment (DO < 1 mg/L [47]) [7,48]. In this case, they will use the available N oxides (NO_2^-, NO_3^- or N_2O) as electron acceptor. However, oxygen rich conditions inhibit the enzymatic reductase of NO_3^- and lead to its accumulation [47,48]. This was noticed in R-2 (period I, Fig. 8) and it is also in concert with findings of Mei at al. (2019) [26].

Throughout period II, a severe decline in the $RE_{ammonia}$ in R-1 was detected (Fig. 7). This can be related to the switch from SF to real petrochemical condensate and an acute toxicity to the nitrification/denitrification steps could be suspected.

On the other hand, between days 174th and 190th (Fig. 4) the delivery of the polluted condensate with unknown compounds caused a sharp decrease in the feed BOD_5. Around day 174 an intended change in the dosing location of the nutrients from the recirculation loop (Fig. 2) to the bulk of R-1 was also made for a better contact. Within this period, the less biodegradable feed/higher O_2 availability and/or the change in the dosing location of the nutrients increased the $RE_{ammonia}$ from 17 ± 9% to 80 ± 9%.

In terms of denitrification in period II, although the C/N ratio reached its maximum (~18, Fig. 9) this step was hindered and NO_3^- accumulated in R-1. In general, high C/N ratio is expected to increase

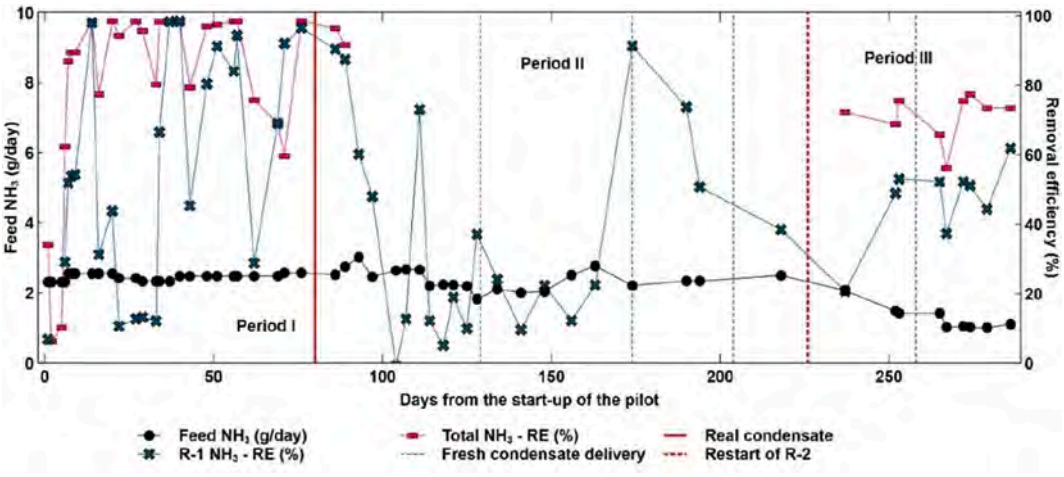

Fig. 7. Ammonia feed load and removal efficiency by the MABR pilot in series versus time from the start-up of the pilot.

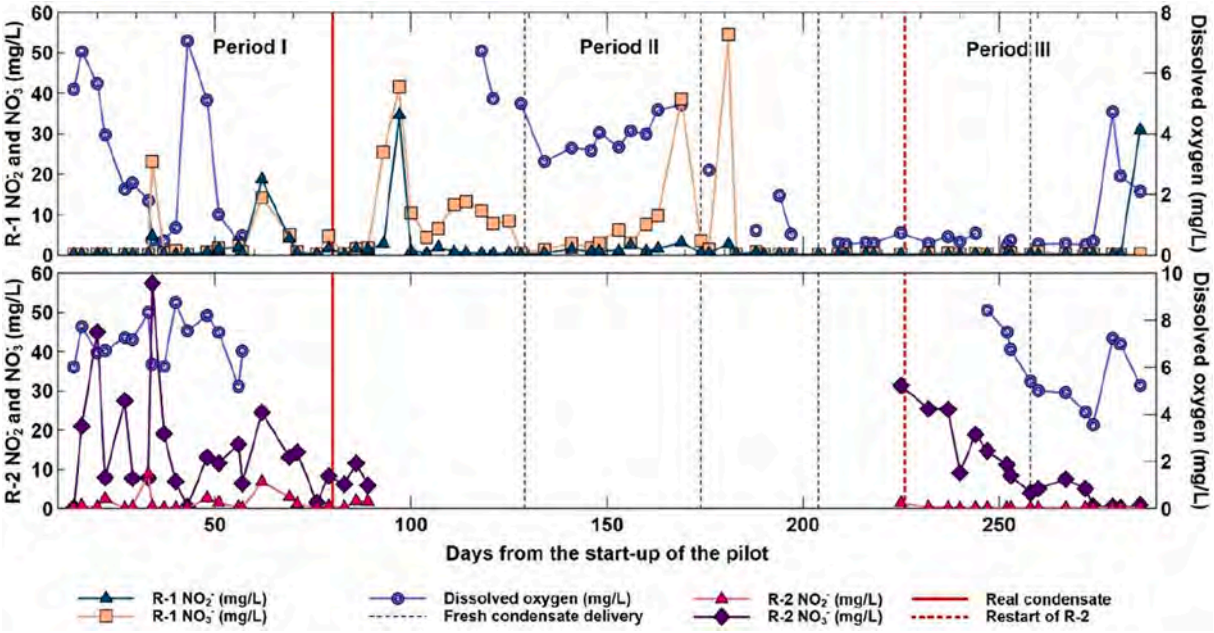

Fig. 8. Concentration of NO_2^-, NO_3^-, and dissolved oxygen profile in each MABR unit – completion of nitrification/denitrification over time from the start-up of the system.

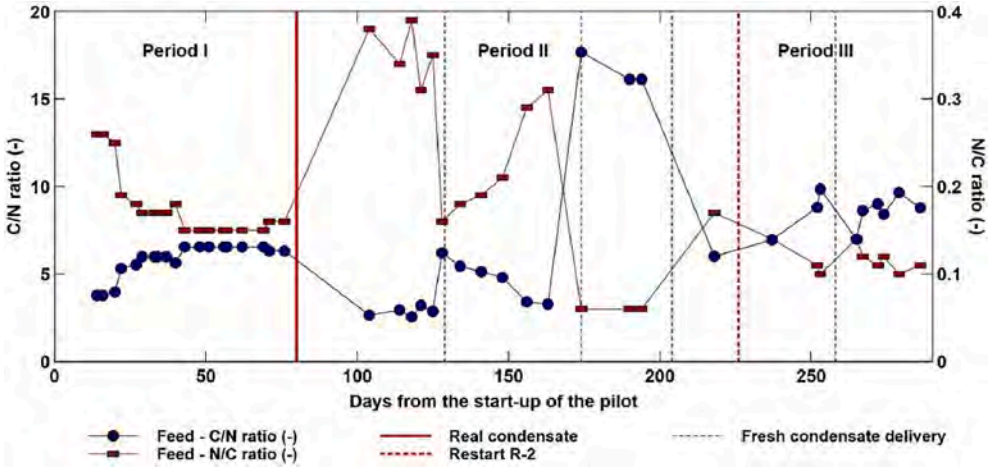

Fig. 9. Carbon/nitrogen and nitrogen/carbon ratios in the feed to the OxyMem MABR pilot versus time from the start-up of the system.

the denitrification efficiency, but the biodegradability of the carbon and the O_2 levels need to be considered. Similar observation was made by Lu et al. (2020) [16], Côté et al. (2015) [18], and Tian et al. (2019) [6].

With more stable feed to the pilot, the operation of R-1 also stabilized (period III, Fig. 8) and no NO_2^-/NO_3^- and DO < 1 mg/L were detected. Such DO values indicated a sufficient biofilm development and membrane coverage (corroborated by [18 41]). The absence of O_2 (or anaerobic conditions) and intermediate byproducts (NO_2^-/ NO_3^-) in the bulk of R-1 pointed towards SND with $RE_{ammonia}$ of 47% ± 11%. Similar $RE_{NH4\text{-}N}$ in a single MABR was noted by P. Li et al. (2015) [5]. In general, the $RE_{NH3/NH4}$ could be optimized by modifying the dosing of nutrients per reactor based on the feed carbon content and its RE in each MABR unit.

With regard to R-2, no accumulation of NO_2^- was observed and with the progressing biofilm development a gradual decrease in NO_3^- was further noted, despite the relatively high DO_{bulk} of 8–3 mg/L (period III, Fig. 8). This can be related to the lower mixing flow rate (413 ± 217 L/h, Table A.4, Appendix A) in R-2 after reinoculation and the presence of suspended biomass in the bulk. Because of that, the formation of dead zones can be expected where O_2 depletion would assure anaerobic denitrification. Nonetheless, variations in the detected DO can be expected until complete membrane coverage, higher mixing rates, and consistent effluent quality are observed.

Besides that, the collected data for R-2 also pointed towards SND at the end of period III and led to an overall $RE_{ammonia}$ of 71 ± 6%. On the other hand, in MABR systems primarily intended to degrade ammonia, RE of ~ 80–99%, >90%, and ~ 92% were reported by Syron et al (2015) [14], Côté et al. (2015) [18], and Q. Li (2018) [20], respectively.

In summary, the possibility for SND (Fig. 1) in the same tank was confirmed. A dependence between the type and the amount of carbon source and the completion of nitrification and denitrification was also observed. Hypothetically, the sharp declines and improvements in the $RE_{ammonia}$ at feed TOC/BOD_5 fluctuations might be an indication for carbon inhibition on the nitrification due to a more direct contact and a different stratification than expected. This requires further research and validation.

3.3.2. Phosphate dosing and removal

During period I, II, and III, the pilot was introduced with on average 1.52 g/day, 1.10 g/day, and 0.44 g/day of PO_4^{3-}. In these three periods $RE_{phosphate}$ in R-1 of 39 ± 31%, 37 ± 28%, and 27 ± 27% and an overall $RE_{phosphate}$ of 44 ± 30%, 47 ± 17% (limited data), and 32 ± 32% was noted.

In general, P contributes to around 3% [49] from the cellular structure of the biomass ($C_{60}H_{87}O_{23}N_{12}P$ [7]). Due to time and equipment limitations, the generated biomass in the pilot and subsequently the consumed P for biomass synthesis was not defined.

3.4. Operational specifics and experiences

3.4.1. Conductivity, pH, temperature, and bulk mixing

The conductivity, pH, and temperature in the feed and in each MABR were regularly monitored (Table A.4, Appendix A). The conductivity in the feed varied around ~ 300 μS/cm for the three tested periods whereas the detected conductivity in R-1 and R-2 was higher (Table A.4, Appendix A). This deviation might originate from accumulation of NO_2^- and NO_3^-, the addition of nutrients, or from the organic pollutants being broken down into charged compounds at the applied pH.

In general, the pH of the petrochemical condensate from the plant was ~ 9.5 ± 0.1 (Table A.1, Appendix A), but gradually decreased in the feed vessels to ~ 7 (Table A.4, Appendix A). Because of that, pH ~ 9 could not be tested at the pilot, but more optimal feed range of 7 was applied and also detected in R-1 and R-2, corroborated by [14,17,24,26].

The temperature was not controlled and corresponded to the ambient conditions, between 15 and 22 °C (Table A.4, Appendix A). Corroborated by [6,20,50,41,26]. Throughout the tested periods, the temperature in R-2 was 1–2 °C higher than in R-1 which was attributed to the heat dissipated by the mixing pumps (Fig. 2).

To achieve high REs in the MABRs external mixing is needed since there is no bubble aerator as in a conventional WWTP. In the OxyMem MABR pilot this was provided by mixing pumps (Fig. 2) and flow rates of 500 L/h (0.32 cm/s) to 1000 L/h (0.62 cm/s) were maintained (Table A.4, Appendix A).

With time, it was observed that the mixing flow rate was directly influenced by the state of the biomass and vice versa. When the membranes were uncovered with biofilm, there was no mechanical resistance to the mixing around them and high rates could be achieved, unlike when covered. For example, R-2 without biofilm (period II, 1127 ± 120 L/h) compared with post-reinoculation (period III, 413 ± 217 L/h) (Table A.4, Appendix A).This is consistent with studies by Nerenberg (2016) [11] and Stricker et al. (2011) [17]. The importance of the fluid velocity to the mass transfer, stratification, and activity of the biofilm in an MABR was also noted by Cole et al. (2004) [42] and Li et al. (2015) [5].

At times, detached biomass got caught in the mixing pumps which reduced the shear and subsequently increased the floating of biosolids. Such issue was tackled by switching off or by deaerating the pumps and it highlights the need for an improved biomass settling. Based on the collected data, it could be concluded that the mixing was highly depended on the state of the biomass and fluctuated with the operational variations. Therefore, occasionally the applied mixing flow rate could be defined as insufficient and further improvement is needed.

3.4.2. Air flow, air pressure, and biofilm scouring

To supply the needed O_2 pressurized air was used (Table A.5, Appendix A). The air flow and pressure to each MABR depended on the certain demand and performance of the biofilm. For instance, more oxygen was needed in R-1 where the majority of the feed carbon was degraded, (~30 L/h, period III, Table A.5, Appendix A) in comparison to R-2 (~10 L/h, period III, Table A.5, Appendix A). At these flow rates, the OTEs achieved by R-1 and R-2 were ~ 21 ± 6% and 34 ± 12%. Corroborated by Syron et al. (2015) [14]. In general, the air flow rate in the fibers can be lowered towards the most optimal OTE as long as the oxygen demand/OTR of the biofilm is still met [14,18]. Such flexibility of the MABR concept allows higher OTEs compared with the CAS process, where maximum of 30% is predicted at testing/clean water conditions [7]. However, such air flow tuning approach was beyond the scope of the current study.

Throughout the testing, the applied air pressure in both MABRs was ~ 150–200 mbars (corroborated by Syron et al. (2015) [14]). The system was equipped with only one off-gas analyzer which recorded mainly values from R-1 of ~ 15–18% O_2 and 0.5–2% CO_2 (Table A.5, Appendix A). The detected difference between this O_2/CO_2 ratio and the starting point of 19/0% (Table 2) indicates an active biofilm or aerobic respiration [7,8]. Comparable O_2 fraction (12–16%) in the exhaust air was reported by Côté et al. (2015) [18].

Once the biofilm covered the membranes and its thickness increased, air scouring through the installed blowers was initiated for biofilm thickness control (Fig. 2). The removed biomass from the fibers ideally settled at the bottom of the reactors and it was discharged from the "scoured biosolids" lines (Fig. 2). If the settling was insufficient, the scoured biomass with time would overflow from the pilot. This biofilm thickness control technique also was utilized by Tian et al. (2019) [6], Sticker et al. (2011) [17] , Syron et al. (2015) [14], and Côté et al. (2015) [18]. Additionally, in the current study an unforeseen drop in the RE of easily biodegradable compounds e.g., acetate or a decrease in the mixing flow rate was used as an indicator for a too thick biofilm. This was related to a mass transfer and diffusion limitation of the pollutant in the biofilm (Fig. 1) and/or a mechanical resistance to the mixing shear. Based on that, scouring also was initiated.

4. Efficiency of the MABR and the CAS concepts – general comparison

4.1. Process configuration and treatment efficiency

Because of their complexity petrochemical waste streams (Table A.1, Appendix A) are treated in WWTPs where initially an equalization step, primary, and secondary oil/water separation are applied. This step is usually followed by a CAS process [8,33]. This is a biological treatment step which consists of fixed bed (biofilters or trickling filters) or in the majority of the cases of suspended bed (activated sludge) processes. In this stage, the soluble substances from the previous steps are adsorbed, absorbed, and assimilated by the biomass. Here, nitrification (aerobic) and denitrification (anaerobic) take place followed by clarification systems (gravity clarifiers, gas floatation) [8,33]. At the biological treatment stage, additional nutrients are often introduced to accomplish the most optimal C: N: P (100:5:1) ratio [33]. Comparably, in an MABR configuration, if not sufficient, N and P sources would be added as well.

When comparing the performance of the researched MABRs in series (Fig. 2) to the CAS process, similar REs of TOC/COD (80–85%), BOD_5 (~95%), phenol (~98%), and NH_3 (~70–90%) were noted. In general, in the CAS process RE of 90–98% for BOD_5 [8,33], 80–90% for COD/TOC, 70–80% for N through nitrification/denitrification, and > 95% for mono aromatic hydrocarbon/phenol with well-adapted biomass were reported [8].

4.2. Aeration – OTR, OTE, SAE, and stripping of VOCs

In the current research, the OTR, OTE, and SAE were calculated for the most representative phase (period III) when both reactors were active and treated the real petrochemical condensate. To calculate these values eqs. (2), 3, and 4 were used and the collected data was tabulated in Table A.3, Appendix A.

In terms of OTR, values for R-1 and R-2 of 2 ± 0.4 g O_2/m^2/day and 1.5 ± 0.5 g O_2/m^2/day were noted (corroborating findings of Stricker et al. (2011) [17]). Such amount of supplied oxygen also was very close to the theoretical demand of R-1 and R-2 of 2.7 ± 0.4 g O_2/m^2/day (eq.

(5)) and 1.1 ± 0.1 g O_2/m^2/day (eq. (6)) (Table A.6, Appendix A). In the estimation of the theoretical oxygen demand the fraction of C and N utilized for biomass production was not included. Thus, lower real oxygen demand than the theoretical might be expected.

The value for OTE detected in R-1 varied around 21 ± 6% and in R-2 around 34 ± 12%. This also was a confirmation of the expected higher OTEs (R-2, 34% > R-1, 21%) at lower air flow rates (R-2, ~10 L/h < R-1, ~30 L/h) (see section 3.4.2). Though, they were very close to the maximum $OTE_{standard\ conditions}$ of CAS (bubble diffusers 4–30% [7,12,15]), which is expected to be even lower in process conditions due to clogging of the aerator's openings [7]. Since in the MABR process the biomass and the aerator/membrane are in constant and direct contact, higher OTE values (30–40% [17,18,19] up to 70–100% [11,14,16,20]) can be reached by tuning the air flow rates [14,18].

The aeration in WWTPs was defined as the most energy-intensive process resulting in ~ 45–75% of the plant operating costs [14,15,51]. Typically, CAS bubble diffusers (fine, medium, and coarse) have reported AE of ~ 0.6–2 kg O_2/kWh [7,51]. In comparison, the values calculated for R-1 and R-2 varied around 6.5 ± 0.2 kg O_2/kWh and ~ 11 ± 0.3 kg O_2/kWh. Overall, the MABR concept was characterized with much higher process energy efficiency than CAS ranging from 3 to 5 [18] to > 10 kg O_2/kWh [14], including the present study (Table A.3, Appendix A).

In general, it is expected that the nature, the biodegradability, C/N ratio, and the amount of the pollutants would directly influence the OTR, OTE, and energy efficiency of an MABR system since it is based on a diffusion/biofilm demand principle [9,14,15,27].

5. Conclusions

A real petrochemical condensate was treated directly via two MABRs in series, each with an HRT of 10 h. At stable operation, the pilot in series achieved an overall/total RE for TOC, BOD_5, organic acids, phenol, and ammonia of 80–85%, ~95%, >98%, ~98%, and 70–90%, respectively. Under stable process conditions the MABR pilot developed a biofilm capable of C and N removal and of conducting simultaneous nitrification/denitrification without traces of intermediate by-products, NO_2^- and NO_3^-. The RE of TOC/COD, BOD_5, phenol, and NH_3-N achieved through the MABR in series was comparable to the RE's accomplished via a CAS: 80–90%, 90–98%, >95%, 70–80% [8,33]. Macro and micronutrients would be externally added during both types of treatment if they are insufficient.

With regard to the energy efficiency, the MABR pilot reached values for OTR, OTE, and SAE of > 1.5 g/m^2/day, > 21%, and > 6.5 kg O_2/kWh. Based on the collected data from the pilot and considering the reported literature findings, this concept can be defined with a potential for a higher energy efficiency compared to the CAS.

In terms of performance stability, MABR-1 individually and particularly in sequence with MABR-2 was able to handle shock loads and feed fluctuations of TOC, ammonia, and organic acids. Such process variations are typical for real petrochemical plants and can be tackled by the rich microbial abundance in the MABR biofilm. This is also beneficial when treating highly recalcitrant substances such as phenol. The second MABR unit provided a treatment buffer capacity to shock loads, which could be an advantage compared with the CAS process.

The main novelty of this paper lies in the fact that the majority of previously reported studies have treated synthetic steams via a lab-scale MABR system, in contrast to the present paper where a real petrochemical condensate was treated in a pilot MABR. Thus, more realistic operational conditions and fluctuations could be experienced. With the gained knowledge and observations from this pilot trial, the MABR concept can be defined as promising for treatment of real petrochemical streams and appealing for future investigations.

Declaration of Competing Interest

The authors declare that they have no known competing financial interests or personal relationships that could have appeared to influence the work reported in this paper.

Acknowledgements

This study was executed within the Institute for Sustainable Process Technology (ISPT) under the scope of the "Steam and Condensate Quality Water Process Technology" project. This project is also co-funded with subsidy from Topsector Energy of the Ministry of Economic Affairs and Climate Policy with project reference TEEI116068. The authors would like to express deepest gratitude to both funding partners.

We would like to also express our genuine appreciation to our colleagues and partners within the ISPT project for their support, feedback, and shared knowhow about the theoretical and practical aspects of the process.

The authors would like also to express sincere gratitude to the laboratory technicians and analytical chemists who performed the analyses, and all provided us with their unconditional assistance.

Appendix A. tables

Table A1
Composition of the real process condensate stream from a petrochemical site. The main parameters mentioned in the table are defined analytically and represent average values. Exceptions are the values obtained at process conditions, *.

Characteristics	Units	Values
TOC	mg/L	100 ± 15
COD		395 ± 122
BOD_5		154 ± 16
TN		8.8 ± 0.9
NH_3		4.7 ± 1.4
PO_4^{3-}		0.5 ± 0.08
Acetate		89.2 ± 81.2
Propionate		8.6 ± 1.5
Formate		5.5 ± 6.8
Phenol		35.8 ± 4.7
BTEX	ppb	3 ± 0.4
Conductivity	μS/cm	285 ± 34
pH	–	~ 9.5 ± 0.1
Flow rate*	mt/h	~ 200
Temperature in processes*	°C	~ 130

*- values at process conditions.

Table A2
Main process parameters and OxyMem MABR membranes specifications.

Total flow rate (L/day)	~ 128
HRT per reactor (h)	~ 10
Volume per reactor (L)	~ 54
Membrane material	polydimethylsiloxane (PDMS) - Silicon
Outer diameter (μm)	510
Inner diameter (μm)	300
Fiber's length (cm)	~ 90
Number of cassettes per reactor (-)	5
Number of bundles per cassette (-)	5
Membrane fibers per bundle (-)	550
Total number of membranes per reactor (-)	13 750
Membrane area per reactor (m^2)	20
Total membrane area of the pilot (m^2)	40
Specific surface area of membrane/volume (m^2/m^3)	364

Table A3
Overview of OTR, OTE, and SAE values of MABR systems reported in literature and obtained from the current MABR pilot study case.

References		Scale and wastewater type	Feed specifics	OTR (g O_2/m^2/day)	OTE (%)	SAE (kg O_2/kWh)
Côté et al. (2015) [18]		Pilot-scale, Municipal primary effluent	10.6–33.4 (mg NH_4-N/L) 98–440 (mg COD/L)	8 – 15	30 – 40	3 – 5, potential 6
Syron et al. (2015) [14]		Pilot-scale, Landfill leachate	500–2500 (mg NH_4/L) 1000–3000 (mg COD /L)	6 – 30	74 - air	10
Li et al. (2018) [20]		Pilot-scale, Municipal primary effluent	9.92–26.60 (mg NH_4-N /L) ~ 130 (mg COD /L)	6.3 – 13.2	24 – 69	x
Houweling et al. (2017) [19]		5 pilot scales, municipal primary effluent and return activated sludge	Mainly for nitrification with rate of 2–3 (g N/m^2/day)	8.7 – 10.8 average of 5	29 – 40	x
Kunetz et al. (2016) [41]		Pilot-scale, Diluted municipal sewage with some industrial contribution	3 – 10 (g N/m^2/day) 6.2 (mg BOD_5 /L) C/N ratio of 0.7	8 – 12	x	3.6 – 7.0, estimated
Stricker et al. (2011) [17]		Pilot-scale, Synthetic feed mimicking effluent of chemical plant – glycerol and NMP	3.6 (g COD/m^2/day) 0.03 (g N/g COD) 6.5–7.8 (g COD/m^2/day)	2.9 x	20 – 40 60–80	x x
The current study, period III	R-1	Pilot-scale, real petrochemical condensate	0.3–2 (g TOC/m^2/day) (*)0.05–0.14 (g NH_3/m^2/day) (*)0.01 – 0.08 (g N/g COD)	2 ± 0.5	21 ± 6	6.5 ± 0.2
	R-2			1.5 ± 0.5	34 ± 12	~ 11 ± 0.3 (#)

x – data not reported; * – data per 20 m^2 of R-1; # – limited data points

Table A4
Average of main operational parameters in the storage tanks and both MABRs - conductivity, pH, temperature, mixing flow rate, and up-flow velocity during the three tested periods.

Average values		Period I			Period II			Period III		
		Feed	R-1	R-2	Feed	R-1	R-2	Feed	R-1	R-2
Conductivity (μS/cm)		289	470	x	306 ± 61	422 ± 129	361 ± 12	274 ± 14	305 ± 49	291 ± 22
pH		7.5 ± 0.4	7.1 ± 0.5	7.8 ± 0.2	7.5 ± 0.7	7 ± 0.3	6.5 ± 0.1	7.4 ± 1	7 ± 0.1	6.7 ± 0.1
Temperature (°C)		x	x	x	15 ± 2	19 ± 1	21 ± 0.8	19 ± 0.5	21 ± 0.9	22 ± 0.7
Mixing flow rate	**(L/h)**	x	827 ± 257	649 ± 370	x	973 ± 38	1146 ± 357	x	1126 ± 120	413 ± 217
Up-flow velocity	**(cm/s)**	x	0.5 ± 0.2	0.4 ± 0.2	x	0.6 ± 0.02	0.7 ± 0.2	x	0.7 ± 0.07	0.3 ± 0.1

x – data not available.

Table A5
Aeration specifications in both MABR units for the three tested periods.

Average values	Period I				Period II				Period III			
	R-1		R-2		R-1		R-2		R-1		R-2	
	In	Out	In	Out	In	Out	In	Out	In	Out	In	Out
Air flow (L/h)	11.5 ± 2.2	8.6 ± 0.8	14 ± 0.6 3.9 ± 0.2 20.5 ± 0.2	x	23 ± 4	21 ± 5	18.4 ± 6.3	11 ± 8.8	32 ± 2	30 ± 0.3	10.5 ± 1.5	10 ± 0.1
Air press. (mbars)	175 ± 18	171 ± 18	157 ± 1.6	142 ± 9.9	210 ± 3.6	204 ± 4.2	202 ± 11	176 ± 21	210 ± 8.5	205 ± 8.4	207 ± 8.9	195 ± 8
Off gas O_2/CO_2 (%)	14.8 ± 1/1.9 ± 0.8		17.6 ± 1.6 /0.5 ± 0.2		16.5 ± 1.3 /1.1 ± 0.4		x		17.6 ± 0.6 /1.5 ± 0.4		x	

x – data not available.

Table A6
Load of main components and corresponding oxygen demand. Total theoretical oxygen demand in R-1 and R-2 - excluding C and N for biomass production.

Days from the start	Oxygen demand based on the load to R-1 and RE in R-1, together ≅ Feed to R-2						TN R-2	Carbon used for denitrification (g COD/m^2/day)		Total theoretical oxygen demand (g O_2/m^2/day)	
	COD/O_2 (g/m^2/day) (#)	RE_{COD} (%)	NH_3-N/O_2 (g/m^2/day) (*)	RE_{NH3-N} (%)	TN load g/m^2/day	RE_{TN} (%)	$RE_{TN,\ R-2}$ (%)	R-1 (**)	R-2 (**)	R-1 (#*)	R-2 (#**)
237	2.9	71.3	0.4	20.7	0.11	3.5	18.7	0.02	0.1	3.3	1
252	3.0	59.8	0.3	48.9	0.09	33.5	x	0.15	0.15	3.2	1.2
253	3.1	x	0.3	53	0.08	19.4	30	0.08	0.08	3.3	x
267	2.2	60.9	0.3	52.2	0.06	30.7	x	0.1	x	2.4	x
272	2.3	56	0.2	37.3	0.06	40.6	16.7	0.13	0.03	2.4	1.1
274	2.2	50.6	0.2	52.3	0.06	40.6	33.3	0.13	0.06	2.2	1.1
279	2.2	45.5	0.2	51	0.06	23.3	42.9	0.07	0.1	2.4	1.2
281	2.2	45.3	0.2	44.3	0.07	37	42.9	0.13	0.1	2.3	1.2
286	2.3	62.2	0.2	61.9	0.07	41.5	16.7	0.14	0.03	2.4	0.9
Avg.	2.5 ± 0.4	56.5 ± 8.4	0.2 ± 0.06	46.8 ± 11	0.07 ± 0.01	30 ± 12	28.7 ± 10.8	0.10 ± 0.04	0.08 ± 0.04	2.7 ± 0.4	1.1 ± 0.1

– 1 (k)g O_2/ 1 (k)g COD; * – 4.57 g O_2/gNH_3-$N_{removed,\ nitrification}$; ** – 5 g COD/g$N_{removed,\ denitrification}$; #* - calculated with eq. (5); #** - calculated with eq. (6); x – data not available.

Table A7
Average composition of the feed for each tested period.

Characteristics	Units	Period I (*)	Period II	Period III
TOC	mg/L	73 ± 31	108 ± 76	103 ± 14
BOD_5		136 ± 70	125 ± 34	165 ± 25
TN		16 ± 1	8 ± 1.5	9.5 ± 1.6
NH_3		20 ± 1	5 ± 1	6.5 ± 1.5
NO_2^-		x	~ 0.2	~ 0.2
NO_3^-		x	~ 0.2	~ 0.2
PO_4^{3-}		9.6 ± 0.4	0.5 ± 0.1	0.5 ± 0.1
Acetate		143 ± 64	65 ± 54	57.2 ± 15.2
Propionate		15 ± 14	8.6 ± 5.4	9.8 ± 2.2
Formate		x	7.5 ± 8.2	3.4 ± 2.5
Phenol		13 ± 11	30.4 ± 6.4	38 ± 7

*- period I, synthetic feed with stepwise increase in carbon load; x – data not available.

Appendix B. detailed analytical methodology

B.1. Total organic carbon (TOC)

To determine the TOC content of the samples, the total inorganic carbon (TIC) was subtracted from the total carbon (TC, organic and inorganic) content. TC was defined by complete oxidation at 680 °C to CO_2, which was quantified in a non-dispersive-infra-red (NDIR) gas analyzer (Shimadzu, TOC-L CPH/CPN, Kyoto, Japan). The TIC fraction (carbonates/bicarbonates) was determined by injecting the sample in acidic solution where carbonate/bicarbonate was converted to CO_2. Afterwards, the CO_2 was sparged from the solution and quantified in a NDIR gas analyzer (Shimadzu, TOC-L CPH/CPN, Kyoto, Japan). The LLD of the equipment was 1 mg/L. Reference method NEN-EN 1484 [36].

B.2. Total nitrogen (TN)

TN was determined by the TNM-L total nitrogen unit which is an additional chemiluminescence based detector on the Shimadzu TOC-L instrument. During the catalytic combustion of organics for TC analysis, free NH_3, NH_4^+, NO_2^-, NO_3^-, and N bounded in the organics was converted to nitrogen oxides (NO). After the CO_2 fraction is detected via the NDIR gas analyzer, the gas is passed through the nitrogen module where NO was mixed with ozone (O_3) and formed NO_2* (*- exited state). When the unstable NO_2* relaxes to its ground state (NO_2), energy is given of as light ($h\nu$). A chemiluminescence detector was used to convert the light to an electronic signal for quantitation of the 'bounded' N. Reference method: NEN-EN 12260:2003 [37].

References

[1] W. Raza, J. Lee, N. Raza, Y. Luo, K.-H. Kim, J. Yang, Removal of phenolic compounds from industrial waste water based on membrane-based technologies, J. Ind. Eng. Chem 71 (2019) 1–18.
[2] M.H. El-Naas, J.A. Acio, A.E.E. Telib, Aerobic biodegradation of BTEX: Progresses and Prospects, J. Ind. Eng. Chem 2 (2014) 1104–1122.
[3] M. El-Naas, Aerobic biodegradation of phenols: A comprehensive review, Critical Rev. Environ. Sci. Technol. 42 (2012) 1631–1690.
[4] A. Bahadori, Pollution Control in Oil, Gas, and Chemical Plants, Springer International Publishing Switzerland (2014) 1–317.
[5] P. Li, D. Zhao, Y. Zhang, L. Sun, H. Zhang, M. Lian, B. Li, Oil-field wastewater treatment by hybrid membrane-aerated biofilm reactor (MABR) system, Chem. Eng. J. 264 (2015) 595–602.
[6] H. Tian, Y. Hu, X. Xu, M. Hui, Y. Hu, W. Qi, H. Xu, B. Li, Enhanced wastewater treatment with high o-aminophenol concentration by two-stage MABR and its biodegradation mechanism, Bioresource Technology 289 (2019) 121649.
[7] M.v. Sperling, Basic Principles of Wasteter treatment - Biological Wasetwater Treatment Series, IWA (2007).
[8] P. Barthe, M. Chaugny, S. Roudier and L. Delgado Sancho, "Europen Commission Science HUB - The European Commission's science and knowledge service. Best Available Techniques (BAT) Reference Document for the Refining of Mineral Oil and Gas. Industrial Emissions Directive 2010/75/EU," 2015. [Online]. Available: https://ec.europa.eu/jrc/en/publication/eur-scientific-and-technical-research-reports/best-available-techniques-bat-reference-document-refining-mineral-oil-and-gas-industrial. [Accessed 16 September 2020].
[9] C. Pellicer-Nàcher, C. Domingo-Félez, S. Lackner, B.F. Smets, Microbial activity catalyzes oxygen transfer in membrane-aerated nitritating biofilm reactors, J. Membr. Sci. 446 (2013) 465–471.
[10] K.J. Martin, R. Nerenberg, The membrane biofilm reactor (MBfR) for water and wastewater treatment: Principles, applications, and recent developments, Biores. Technol. 122 (2012) 83–94.
[11] R. Nerenberg, The membrane-biofilm reactor (MBfR) as a counter-diffusional biofilm process, Current Opin. Biotechnol. 38 (2016) 131–136.
[12] D. Rosso, R. Iranpour, M.K. Stenstrom, Fifteen years of offgas transfer efficiency measurements on fine-pore aerators: Key ROLE OF SLUDGE AGE AND NORMALIZED AIR FLux, Water Environ. Res 77 (3) (2005) 266–273.
[13] M. Bajaj, C. Gallert, J. Winter, Biodegradation of high phenol containing synthetic wastewater by an aerobic fixed bed reactor, Bioresource Technology 99 (2008) 8376–8381.
[14] E. Syron, M.J. Semmens, E. Casey, Performance analysis of a pilot-scale membrane aerated biofilm reactor for the treatment of landfill leachate, Chem. Eng. J. 273 (2015) 120–129.
[15] M. Aybar, G. Pizarro, J. Boltz, L. Downing, R. Nerenberg, Energy-efficient wastewater treatment via the air-based, hybrid membrane biofilm reactor (hybrid MfBR), Water Sci. Technol 69 (8) (2014) 1735–1741.
[16] D. Lu, H. Bai, F. Kong, S.N. Liss, B. Liao, Recent advances in membrane aerated biofilm reactors, Critical Rev. Environment. Sci. Technol. 51 (7) (2021) 649–703.
[17] A. Stricker, H. Lossing, J.H. Gibson, Y. Hong, J.C. Urbanic, Pilot scale testing of a new configuration of the membrane aerated biofilm reactor (MABR) to treat high-strength industrial sewage, Water Environ. Res. 83 (1) (2011) 3–14.
[18] P. Côté, J. Peeters, N. Adams, Y. Hong, Z. Long, J. Ireland, A new membrane-aerated biofilm reactor for low energy wastewater treatment: Pilot results, Water Technol. Solut. Tech. Rep. 2015 (13) (2015) 4226–4239.
[19] D. Houweling, J. Peeters, P. Cote, Z. Long, N. Adams, Proving membrane aerated biofilm reactor (MABR) performance and reliability: Results from four pilots and a full-scale plant, Water Environment Federation 2017 (16) (2017) 272–284.
[20] Q. Li, "Master Thesis: Pilot-scale plant application of membrane aerated biofilm reactor (MABR) technology in wastewater treatment," KTH Royal institute of Technology School of Architecture and the built Environment, 2018.
[21] E. Syron, E. Casey, Membrane-aerated biofilms for high rate biotreatment: performance appraisal, engineering principles, scale-up, and development requirements, Environmental Sci. Technol. 42 (2008) 1833–1844.
[22] Y. Li, K. Zhang, Pilot scale treatment of polluted surface waters using membrane-aerated biofilm reactor (MABR), Biotechnol. Biotechnol. Equip. 32 (2) (2018) 376–386.
[23] E. Syron, H. Kelly, E. Casey, Studies on the effect of concentration of a self-inhibitory substrate on biofilm reaction rate under co-diffusion and counter diffusion configurations, J. Membr. Sci. 335 (1-2) (2009) 76–82.
[24] T. Li, J. Liu, R. Bai and F. Wong, "Membrane-Aerated Biofilm Reactor for the Treatment of Acetonitrile Wastewater," Environ. Sci. Technol, no. 42, pp. Environ. Sci. Technol. 2008, 42, 2099–2104, 2008.
[25] M. Lan, M. Li, J. Liu, X. Quan, Y. Li, B. Li, Coal chemical reverse osmosis concentrate treatment by membrane-aerated biofilm reactor system, Biores. Technol. 270 (2018) 120–128.
[26] X. Mei, J. Liu, Z. Guo, P. Li, S. Bi, Y. Wang, Y. Yang, W. Shen, Y. Wang, Y. Xiao, X. Yang, B. Zhou, H. Liu, S. Wu, Simultaneous p-nitrophenol and nitrogen removal in PNP wastewater treatment: Comparison of two integrated membrane-aerated bioreactorsystems, J. Hazard. Mater. 363 (2019) 99–108.
[27] O. Hanay, E. Taskan, B. Yildiz, H. Hasar and E. Casey, "Gas/Substrate Fluxes and Microbial Community in Phenol Biodegradation Using an O2-Based Membrane Biofilm Reactor," Clean - Soil, Air, Water, pp. 1-7, 2013.
[28] A. Klindworth, E. Pruesse, T. Schweer, J. Peplies, C. Quast, M. Horn, F.O. Glöckner, Evaluation of general 16S ribosomal RNA gene PCR primers for classical and next-generation sequencing-based diversity studies, Nucleic Acids Res. 41 (1) (2013) e1.
[29] P. D. Schloss, D. Gevers and S. L. Westcott, "Reducing the Effects of PCR Amplification and Sequencing Artifacts on 16S rRNA-Based Studies," Plos ONE, vol. 6, no. 12, 2011.
[30] J. J. Kozich, S. L. Westcott, N. T. Baxter, S. K. Highlander and P. D. Schloss, "Development of a Dual-Index Sequencing Strategy and Curation Pipeline for Analyzing Amplicon Sequence Data on the MiSeq Illumina Sequencing Platform," Applied and Environmental Microbiology, pp. 5112-5120, 2013.
[31] B. Cao, X. Lyu, C. Wang, S. Lu, D. Xing, X. Hu, Rational collaborative ablation of bacterial biofilms ignited by physical cavitation and concurrent deep antibiotic release, Biomaterials 262 (2020) 120341.
[32] M.E. Davis, R.J. Davis, Fundamentals of Chemical Reaction Engineering, McGraw-Hili, New York, 2003.
[33] S. Jafarinejad, S.C. Jiang, Current technologies and future directions for treating petroleum refineries and petrochemical plants (PRPP) wastewaters, J. Environm. Chem. Eng. 7 (5) (2019) 103326.
[34] P.S. Davies, The Biological Basis of Wastewater Treatment, Strathkelvin Instruments Ltd, Glasgow, 2005, p. 2005.
[35] L. Thompson, V. Gray, D. Lindsay, A. von Holy, Carbon : Nitrogen : Phosphorus ratios influence biofilm formation by Enterobacter cloacae and Citrobacter freundii, J. Appl. Microbiol 101 (2006) 1105–1113.
[36] T. R. N. S. Institute, "NEN-EN 1484, Water Analysis - Guidlines for the determination of Total Organic Carbon (TOC) and Dissolved Organic Carbon (DOC)".
[37] T. R. N. S. Institute, "NEN-EN 12260 : 2003: "Water quality - Determination of nitrogen - Determination of bound nitrogen (TN sub b), following oxidation to nitrogen oxides"".

[38] T. C. C. 2. ". Analysis", "Europen Standard, NEN-EN-1899-1: Determination of the Biochemical Oxygen Demand after n days. Part 1: Dilution and engrafting under additive of allylthiourea," 1998.
[39] P. Côté, J.-L. Bersillon, A. Huyard and G. Faup, "Bubble-free aeration using membranes: process analysis," Journal Water Pollution Control Federation, vol. 60, no. 11, 1988.
[40] W. Byrne, "Design Your Own MABR," OxyMem a DuPont brand, 2017-2019. [Online]. Available: https://www.oxymem.com/blog/design-your-own-mabr. [Accessed 1 February 2021].
[41] T. E. Kunetz, A. Oskouie, A. Poonsapaya, J. Peeters, N. Adams, Z. Long and P. Cote, "Innovative Membrane-Aerated Biofilm Reactor Pilot Test to Achieve Low-energy Nutrient Removal at the Chicago MWRD," Proceedings of the Water Environment Federation, 2016.
[42] A. C. Cole, M. J. Semmens and T. M. LaPara, "Stratification of Activity and Bacterial Community Structure in Biofilms Grown on Membranes Transferring Oxygen," Applied and Environmenta; Microbiology, vol. 70, no. 4, pp. 1982-1989, 2004.
[43] X. Mei, Y. Wang, Y. Yang, L. Xu, Y. Wang, Z. Guo, W. Shen, Z. Zhang, M. Ma, Y. Ding, Y. Xiao, X. Yang, C. Yin, W. Guo, K. Xu, C. Wang, Enhanced treatment of nitroaniline-containing wastewater by a membraneaerated biofilm reactor: Simultaneous nitroaniline degradation and nitrogen removal, Sep. Purificat. Technol. 248 (2020) 117078.
[44] C.M. Potvin, Z. Long, H. Zhou, Removal of tetrabromobisphenol A by conventional activated sludge, submerged membrane and membrane aerated biofilm reactors, Chemosphere 89 (2012) 1183–1188.
[45] S. Navada, M. F. Knutsen, I. Bakke and O. Vadstein, "Nitrifying biofilms deprived of organic carbon show higher functional resilience to increases carbon supply," Scientific Reports, (2020).
[46] K. Bernat, I. Wojnowska-Baryła, Carbon source in aerobic denitrification, Biochem. Eng. J. 36 (2) (2007) 116–122.
[47] X. Zhang, J. Zhang, Effect of dissolved oxygen on biological denitrification using biodegradable plastic as the carbon source, Earth Environ. Sci. 121 (2018) 032015.
[48] U. Skiba, "Denitrification," in Encyclopedia of Ecology, 2008, pp. 866-871.
[49] M.H. Gerardi, Wastewater Bacteria, John Wiley & Sons Inc, Hoboken, New Jersey, 2006.
[50] T. Li, J. Liu, Factors affecting performance and functional stratification of membrane-aerated biofilms with a counter-diffusion configuration, Faraday Discuss. R. Soc. Chem 9 (2019) 29337–29346.
[51] D. Rosso and M. K. Stenstrom, "Energy-saving benefits of denitrification," Environmental Engineer: Applied Research & Practice, vol. 3, 2007.